ENVIRONMENTAL RESEARCH
LETTERS

LETTER • **OPEN ACCESS**

Wind amplifies the polar sea ice retreat

To cite this article: Ramdane Alkama *et al* 2020 *Environ. Res. Lett.* **15** 124022

Environmental Research Letters

LETTER

Wind amplifies the polar sea ice retreat

Ramdane Alkama[1,*], Ernest N Koffi[1], Stephen J Vavrus[2], Thomas Diehl[1], Jennifer Ann Francis[3], Julienne Stroeve[4], Giovanni Forzieri[1], Timo Vihma[5] and Alessandro Cescatti[1]

[1] European Commission, Joint Research Centre, Ispra, Italy
[2] Nelson Institute Center for Climatic Research, University Wisconsin-Madison, Madison, WI 53706, United States of America
[3] Woods Hole Research Center, Falmouth, MA, United States of America
[4] University College London, Centre for Polar Observation and Modelling, London, United Kingdom
[5] Finnish Meteorological Institute, Helsinki, Finland
[*] Author to whom any correspondence should be addressed.

E-mail: ram.alkama@hotmail.fr

OPEN ACCESS

RECEIVED
2 July 2020

REVISED
6 October 2020

ACCEPTED FOR PUBLICATION
21 October 2020

PUBLISHED
30 November 2020

Keywords: polar sea ice, wind speed, poleward transfer of heat and moisture, thermal, dynamic, turbulent and radiative, local vertical fluxes, large-scale horizontal fluxes

Supplementary material for this article is available online

Abstract

The rapid polar sea ice retreat and its drivers are challenging and still unresolved questions in climate change research. In particular, the relationship between near-surface wind speed and sea ice extent remains unclear for two main reasons: (1) observed wind speeds over Polar Regions are very sparse, and (2) simulated winds by climate models are dependent on subjective parameterizations of boundary layer stratification, ultimately leading to large uncertainty. Here, we use observation-based data (passive microwave sea ice concentration and six different reanalysis datasets) together with output from 26 climate models (from the CMIP5 archive) to quantify the relationships between near-surface wind speed and sea ice concentration over the past 40 years. We find strong inverse relationships between near-surface wind speed and sea ice concentration that are consistent among the six reanalysis datasets. The poleward wind component is particularly increasing in years of reduced sea ice concentration, which contributes to the enhancement of the atmospheric (surface oceanic) poleward heat flux by up to 24 $\pm$ 1% (29 $\pm$ 2%) in the Arctic and 37 $\pm$ 3% (51 $\pm$ 3%) in the Antarctic seas, therefore boosting the impact of polar sea ice loss and contributing to polar amplification of climate warming. In addition, our results show a marginal contribution of the dynamical (pushing/opening/compacting) effects of wind on sea ice compared to the thermodynamic effects which in turn play a lower role than the associated change in local surface Autumn–Winter turbulent and Spring–Summer radiative fluxes. Climate models generally produce similar results but with lower magnitude, and one model even simulates the opposite relationship wind/sea-ice. Given the rapid changes in polar climate and the potential impacts on the mid-latitudes, it is urgent that model developments make use of evidence from satellite observations and reanalysis datasets to reduce uncertainties in the representation of relationships between polar winds and sea ice.

1. Introduction

Polar regions, especially the Arctic, are warming at least twice as fast as the global average (Blunden *et al* 2012), a feature called polar amplification. This accelerating warming is impacting sea ice area, one of the most prominent indicators of climate change (Parkinson 2019). Variation in sea ice area is widely cited as the trigger of the positive feedback responsible for polar amplification (Hansen *et al* 1997, Kirtman *et al* 2013), because the warming-induced reduction of sea ice cover contributes to more absorption of solar radiation by the surface and thus contributes to more warming. However, the largest polar amplification occurs in the cold season, when the ice–albedo effect is zero or small and processes other than albedo accordingly dominate. In particular, sea ice cover change may also affect atmospheric and ocean circulations, which in turn may contribute to polar amplification (Vihma 2014). This does not exclude totally

the role of albedo feedback that can warm the Polar Ocean in the warm seasons and then this can be communicated to the cold season by a reduction in winter sea ice cover which allows the relatively warm ocean to rapidly heat the overlying cold atmosphere. The relevance of these processes goes well beyond the polar zones, since sea ice decline contributes to the amplification of warming in the polar regions and may ultimately affect the entire climate system (Cohen *et al* 2014, England *et al* 2020): rising sea levels with its possible impact on ocean and sea shores (Nicholls and Cazenave 2010), changes in climate and precipitation patterns (Dore 2005), increase of the frequency and intensity of severe weather events (Stott 2016), and its impact on birds, marine mammals and polar bears (Stirling 1997, Smetacek and Nicol 2005).

The causes of such an amplification are still being debated by the scientific community (Maksym 2019). In fact, the direct effect of increasing greenhouse gases alone (excluding atmospheric and oceanic feedbacks) cannot explain the observed rapid sea ice retreat (Comiso *et al* 2008, Maksym 2019). Some authors have suggested the important role of internal variability, in addition to the forced response, on the observed Arctic sea ice trend (Kay *et al* 2011, England *et al* 2019, Ding *et al* 2019). Others have suggested an increased ocean heat transfer to the poles as a potential driver (Chylek *et al* 2009). However, numerous recent studies show a slowing down of poleward ocean heat transport during the last decade (Srokosz and Bryden 2015, Thornalley *et al* 2018, Caesar *et al* 2018), concomitant with the observed acceleration of sea ice retreat (Maksym 2019). This does not exclude completely oceans as potential driver since the top ocean heat transfer, which is different from the total ocean heat transfer, is known to play an important role in Bering and Barents Sea ice retreat (Nakanowatari *et al* 2014, 2015, Sato *et al* 2014). Others have suggested the cloud radiative feedback as a potential driver (Cao *et al* 2017). Indeed, clouds play a warming role by increasing the emission of thermal radiation back to the surface. But clouds may also play a cooling role by reflecting incoming solar radiation to space, and on an annual scale, the cooling role of clouds is dominant, meaning that clouds play a damping role for sea ice retreat rather than an enhancing role on the surface radiative budget (Alkama *et al* 2020). This does not exclude the thermal role of clouds but rather suggests that it moderates the formation of sea ice during winter and then, because of lower surface albedo, solar radiation plays a dominant warming role on the surface radiative budget during summers (Screen and Simmonds 2010), despite the associated cloudier atmosphere that damps partially this effect (Alkama *et al* 2020). Some authors point out a potential role for atmospheric heat transfer (known to partly be driven by wind speed and direction: 'thermodynamic effect of wind') as a potential driver, but unfortunately they did not quantify such an effect on sea ice retreat (Zhang *et al* 2008, Graversen *et al* 2008, Overland and Wang 2010). Other authors find that wind may impact inter-annual variations and seasonal extent of sea ice concentration by contributing to the drift and deformation of sea ice (Rigor *et al* 2002, Rampal *et al* 2009, Jakobson *et al* 2019) ('dynamic effect of wind'). However, these studies generally have not accounted for the thermodynamic effect of wind.

Satellites have provided since 1979 a consistent and continuous record of sea ice concentration (SIC) retrieved from passive microwave radiometer measurements, which can be ideally used to produce an evidence-driven assessment of recent trends and drivers of polar sea ice retreat. Unfortunately, evidence-based studies have been limited by the paucity of *in situ* observations of wind speed (WS) and direction in the Polar Regions. Only a few *in situ* polar datasets exist, which unfortunately do not provide enough coverage in space and time for a robust observation-driven analysis of the interplay between wind and SIC. To overcome this limitation, the use of climate reanalysis is required. Reanalysis datasets are created through data assimilation systems based on numerical weather prediction models constrained by a large number of *in situ* and satellite observations. Reanalyses provide a dynamically consistent estimate of 10 m wind and other atmospheric components that have proved to be highly correlated with observations over the Arctic (correlation around 0.9) (Francis *et al* 2005, Lindsay *et al* 2014, Graham *et al* 2019) and Antarctic (Dong *et al* 2020). To account for the physical uncertainty of reanalyses, we used 10 m wind speed and direction from an ensemble of six different datasets (ERAinterim (Dee *et al* 2011), ERA5 (Hersbach *et al* 2020), NCEP_NCAR (Kalnay *et al* 1996), NCEP_DOE (Kanamitsu 2002), NCEP_CFSR (Saha *et al* 2010) and ASR (Bromwich *et al* 2018); see data and methods section).

As briefly discussed above, wind impacts SIC by: (1) a dynamical effect, by contracting, drifting and deforming sea ice; and (2) a thermodynamic effect, by bringing more atmospheric (Zhang *et al* 2008, Graversen *et al* 2008, Overland and Wang 2010) and surface ocean heat (Nakanowatari *et al* 2014, 2015, Sato *et al* 2014) to the polar regions. Both these large-scale horizontal fluxes effects of wind on SIC, have an impact on the surface albedo, and thus indirectly, have an impact on the local vertical fluxes via surface radiative budget (Screen and Simmonds 2010). Bringing more atmospheric moisture to polar regions is also known to have an important impact on the surface radiative budget (Boisvert *et al* 2013, Vihma *et al* 2016, Woods and Caballero 2016). As an additional local vertical fluxes effect, the transport of heat and moisture to the Polar Regions may impact SIC change via surface turbulent fluxes (Park *et al* 2015b, Woods and Caballero 2016). The first objective of the study is

then to quantify the inter-annual sensitivity between wind speed and SIC over the last 40 years, which has never been quantified before, in both polar seas using 6 different reanalysis datasets and 26 climate models from the CMIP5 archive. The second objective is to study which of the zonal and meridional components of wind dominates this sensitivity and pay particular attention to the meridional (poleward) wind that has a larger potential to bring heat and moisture to the Polar Regions. After studying the wind-SIC sensitivity, the third objective is to understand the direction of causality between them. Is an increase of wind the underlying driver for sea ice loss? Or does the decline in sea ice increase wind with its potential positive feedback on sea ice loss? This will be accomplished using a month-to-month analysis, since it does not make sense to use the inter-annual signal ignoring what is happening in previous months. Finally, we will explore the relative importance of the large-scale horizontal fluxes (dynamic, atmospheric heat flux (ATM), ocean heat flux (OHF)), local vertical fluxes (net surface radiation (NSR) and surface turbulent flux) and both effects of wind on sea ice.

Before discussing the results and the conclusion, we first describe the methods and data used in this work.

2. Methods and data

2.1. Sea ice concentration

Sea ice concentration was computed from satellite passive microwave brightness temperatures from the series of Special Sensor Microwave Imager/Sounder (SSMIS), the Special Sensor Microwave/Imager (SSM/I), and the Scanning Multichannel Microwave Radiometer (SMMR). It provides a consistent, daily and monthly time series of sea ice concentrations from 1978–onwards through the most recent processing for both the North and South Polar Regions. This dataset is produced at the EUMETSAT Satellite Application Facility on Ocean and Sea Ice (OSI SAF) on a 25 km × 25 km grid (https://cds.climate.copernicus.eu/cdsapp#!/dataset/satellite-seaice?tab=overview).

In order to check the robustness of our analysis, the latest Bootstrap_nt and Bootstrap_merged sea ice concentration derived from passive microwave brightness temperatures is also used as a test. These datasets are from the National Snow and Ice Data Center (NSIDC; http://nsidc.org/data/G02202).

2.2. Reanalysis

In the past several years, a number of reanalysis datasets have become available. The six leading datasets used in the current study are described below.

a. *ERAinterim*: This belongs to the European Center for Medium-Range Weather Forecasts (ECMWF) reanalysis series (including ERA-15, ERA-40, ERAinterim (Dee *et al* 2011) and ERA5). ERAinterim uses four-dimensional variational data assimilation (4D-Var) and is run at T255 (nominally 0.70°) horizontal resolution. In addition, data assimilation of ERAinterim benefits from more extensive use of radiances with an improved fast radiative transfer model compared to the previous version ERA-40.
b. *ERA5*: ERA5 (Hersbach *et al* 2020) is the most recent ECMWF reanalysis product. It is based on the Integrated Forecast System (IFS), the main ECMWF global forecasting model. Its horizontal resolution is about 30 km (distributed at 0.25°), it is available from 1979 to the present. Most variables are provided hourly. In addition to wind speed, we also used wind gust, surface pressure, boundary layer height, 2 m air temperature, zonal and meridional wind, surface turbulent flux (surface latent and sensible heat flux), surface net radiation and atmospheric integral of northward kinetic and heat flux. (http://climate.copernicus.eu/climate-reanalysis).
c. *NCEP_NCAR*: The Reanalysis 1 project is using a state-of-the-art analysis/forecast system to perform data assimilation using past data from 1948 to the present. A large subset of this data is available from NOAA in its original 6 hourly format and as daily averages (Kalnay *et al* 1996) (https://www.esrl.noaa.gov/psd/). This product is distributed with a spatial resolution of 2.5 degree latitude × 2.5 degree longitude. (https://www.esrl.noaa.gov/psd/data/gridded/data.ncep.reanalysis.derived.surface.html).
d. *NCEP_DOE*: NCEP-DOE (Kanamitsu 2002) Reanalysis 2 is an improved version of the NCEP_NCAR Reanalysis 1 model that fixed errors and updated parameterizations of physical processes. This product is distributed on a T62 Gaussian grid and is available from 1979 to the present with a 6 hourly temporal resolution. (https://rda.ucar.edu/datasets/ds091.0/).
e. *NCEP_CFSR*: The Climate Forecast System Reanalysis (CFSR) is a global, high resolution (hourly, T382 Gaussian grid ∼38 km), coupled atmosphere-ocean-land surface-sea ice system designed to provide the best estimate of the state of these coupled domains over this period. This product covers the period 1979–2010. Despite the use of a coupled ocean-atmosphere model, the ocean-atmosphere interactions are not used directly. The actual reanalysis is uncoupled. This product is retrieved from (https://climatedataguide.ucar.edu/climate-data/climate-forecast-system-reanalysis-cfsr).
f. *ASR*: The Arctic System Reanalysis (ASR (Bromwich *et al* 2018)) is a multi-agency, university-led retrospective analysis (reanalysis)

of the Greater Arctic. ASR is produced using high-resolution versions of the Polar Weather Forecast Model (PWRF) and the WRF-VAR and High Resolution Land Data Assimilation (HRLDAS) data assimilation systems that have been optimized for the Arctic. ASR is a comprehensive integration of the regional climate of the Arctic, currently for the period 2000–2016. We used the ASRv2 version which is produced at 15 km spatial resolution, 3 hourly temporal resolution and available through the NCAR Research Data Archive. (https://climatedataguide.ucar.edu/climate-data/arctic-system-reanalysis-asr).

2.3. CMIP5 models

We used monthly 10 m wind speed and sea ice concentration from an ensemble of simulations conducted with 26 Earth system models (names of the used models are shown in an animation file, see supplementary materials (available online at https://stacks.iop.org/ERL/15/124022/mmedia)) contributing to the Coupled Model Intercomparison Project Phase 5 (CMIP5) (Taylor *et al* 2012). These model experiments provided: (a) historical runs (1850–2005), in which all external forcings are based on observations; (b) future runs (2006–2100) under RCP8.5 emission scenarios (Taylor *et al* 2012). The comparison with the satellite data is carried out for the period 1979–2018. For this purpose, we merged the historical runs 1979–2005 with the RCP8.5 runs 2006–2018. The difference between RCP8.5 and RCP4.5 over the period 2006–2018 is very limited so the choice of emission pathways should not have a major impact. All models are analyzed on their native atmospheric model grids. SIC is bi-linearly interpolated from the ocean grid (higher resolution) to the atmospheric grid (lower resolution).

In addition to wind speed and SIC, we also used 2 m air temperature of the two extreme models CanESM2 and MRI-CGCM3, since all other models show intermediate sensitivity between wind and sea ice.

2.4. Estimation of the local variation in wind speed from the changes in sea ice concentration

In order to estimate the local variation in wind speed or other variables from the change in SIC, we used the following steps:

1. For a given area, we calculate the wind speed change ΔWS_i, i.e. the differences of wind between two consecutive years. ΔWS_i values are summarized in a schematized plot (figure S1a) where each cell i shows the average ΔWS_i observed for all possible combinations of sea ice concentration in the two consecutive observation years (year yi and yi + 1 from the time period 1979–2018) reported on the X and Y axis, respectively. For the sake of clarity in figure S1 the X and Y axes report sea ice concentration by intervals of 10%, while in the discussed figures the axes are discretized with 2% bins.
2. Because of the regular latitude/longitude grid used in the analysis, the area of the grid cells (a_m) varies with latitude. The energy signal (ΔWS_i) is therefore computed as an area weighted average (equation 1):

$$\Delta WS_i = \frac{\sum_{m=1}^{M} a_m \Delta WS_m}{\sum_{m=1}^{M} a_m}. \quad (1)$$

3. The area weighted average (ΔWS_p) of the energy signal (ΔWS_i) of all (N) grid cells with the same fraction X of change in sea ice concentration (shown with the same colour in figure S1) is calculated as follows (equations 2 and 3):

$$A_i = \sum_{m=1}^{M} a_m \quad (2)$$

$$\Delta WS_p = \frac{\sum_{i=1}^{N} A_i \Delta WS_i}{\sum_{i=1}^{N} A_i}. \quad (3)$$

The average energy signals (ΔWS_p) per class of sea ice concentration change are finally reported in a scatterplot (figure S1 right panel) and used to estimate a regression line with zero intercept.

The slope S of this linear regression represents the local WS energy signal generated by the complete sea ice melting. The weighted root mean square error 'WRMSE' of the slope is estimated by equation (4), where p represents one of the NP points in the scatterplot (figure S1 right panel) and X_p is the relative change in sea ice concentration in the range ± 1 (equivalent to $\pm 100\%$ of sea ice cover change).

$$\mathrm{WRMSE} = \sqrt{\frac{\sum_{p=1}^{NP} A_p \left(\Delta WS_p - SX_p\right)^2}{\sum_{p=1}^{NP} A_p}},$$
$$\text{where } A_p = \sum_{i=1}^{N} A_i. \quad (4)$$

2.5. The vertical integral of northward atmospheric heat flux

The vertical integral of northward atmospheric heat flux as defined in the ERA5 reanalysis dataset that is based on (Oort and Peixóto 1983) (equation below), is a function of the gravity 'g', absolute temperature 'T', specific heat capacity c_p, the northward wind component 'v', atmospheric pressure 'p' and

the vertical hybrid coordinate used within the ERA5 framework 'η'.

$$\frac{1}{g}\int_0^1 v c_p T \frac{\partial p}{\partial \eta} \mathrm{d}\eta.$$

This parameter is the horizontal rate of flow of heat in the northward direction, per meter across the flow, for a column of air extending from the surface of the Earth to the top of the atmosphere. Positive values indicate a flux from south to north.

2.6. The vertical integral of northward kinetic atmospheric flux

The vertical integral of northward atmospheric kinetic flux as defined in the ERA5 reanalysis dataset that is based on (Oort and Peixóto 1983) (equation bellow), is a function of the gravity 'g', the northward wind component 'v', atmospheric pressure 'p' and the vertical hybrid coordinate used within the ERA5 framework 'η'.

$$\frac{1}{g}\int_0^1 v \frac{1}{2} v^2 \frac{\partial p}{\partial \eta} \mathrm{d}\eta.$$

2.7. Northward ocean heat flux

The northward top ocean heat advection (OHF) is computed by multiplying the density ρ and the specific heat of water $c_p$and by vertically integrating over a layer spanning from the surface to 55 m, which we consider as the mixed layer depth (MLD). In reality, MLD has a clear seasonal cycle which can be deeper than 50 m in winter and shallower than 10 m in summer. However, if we assume that MLD is constant for each month of the year, then choosing MLD = 10 m or 55 m does not have any impact on the relative importance method since multiplying a time series by a constant does not have any influence on the results (Grömping 2006). The northward top ocean heat flux as defined in the equation below is used to estimate the relative importance (see section 2.9) for each month of the year of four drivers on SIC.

$$\rho c_p \int_0^{\mathrm{MLD}} v \frac{\partial T}{\partial y} \mathrm{d}z.$$

Here y and z indicate a meridional and vertical axis respectively. T is the sea surface temperature from ERA5 that is mainly based on observations, and 'v' is the northward component of water advection of the top few meters from the ERA5 dataset. In reality, T should represent the average temperature of water over the MLD, but there is an absence of observed mixed MLD temperature data. Therefore, we must use sea surface temperature, which should be close but may suggest a slight overestimation of the OHF.

2.8. Net surface radiation and surface turbulent flux

Net surface radiation (NSR) is the balance between total incoming radiation from the atmosphere and upward-reflected shortwave radiation and emitted longwave radiation from the surface. Surface turbulent flux (Turbulent) is the sum of latent and sensible heat flux at the surface. The NSR and Turbulent used in the current study are taken from the ERA5 dataset.

2.9. Quantifying the relative importance of the dynamic, surface net radiation, atmospheric and oceanic heat transport part of wind on sea ice concentration change

To separate the thermal part of wind from the dynamical, turbulent and the radiative part we used a relative importance index from the R package (Grömping 2006) for the multilinear equation below:

$$\begin{aligned}\Delta\mathrm{SIC} &= \alpha_1 \Delta\,(\text{northward atmospheric heat flux})\\ &+ \alpha_2 \Delta\,(\text{northward ocean heat flux})\\ &+ \alpha_3 \Delta\,(\text{northward kinetic flux})\\ &+ \alpha_4 \Delta\,(\text{net surface radiation})\\ &+ \alpha_5 \Delta\,(\text{surface turbulent flux}).\end{aligned}$$

Here, 'northward atmospheric heat flux' and 'northward kinetic flux' is the northward heat and kinetic flux at 10 m from ERA5, while SIC is taken from observations as described before (section 2.1). Δ refers to the difference of the same month between consecutive years. α_1, α_2, α_3, α_4 and α_5 are constants that are estimated from solving a system of five unknowns and a large number of equations ($39 = 40-1$ years multiplied by the number of grid cells with SIC > 0), using the relative importance index from the R package (Grömping 2006).

$$\begin{aligned}&\text{Atmospheric heat flux } (AHF)\\ &\quad = \alpha_1 \Delta\,(\text{northward atmospheric heat flux})\\ &\text{Ocean heat flux } (OHF)\\ &\quad = \alpha_2 \Delta\,(\text{northward ocean heat flux})\\ &\text{Dynamic part (Dynamic)}\\ &\quad = \alpha_3 \Delta\,(\text{northward kinetic flux})\\ &NSR = \alpha_4 \Delta\,(\text{net surface radiation})\\ &\text{Turbulent} = \alpha_5 \Delta\,(\text{surface turbulent flux}).\end{aligned}$$

In order to estimate the large-scale horizontal fluxes effects of wind on SIC, only the three first (AHF, OHF and Dynamic) terms of the equation are used. However, for the local vertical fluxes effects, only the last two (NSR, Turbulent) terms are accounted. Thus, the full equation accounts for both horizontal and vertical fluxes effects. We have to note here that, when using the full equation, we are making a simple summation of the five effects. However, in reality, the separation between the horizontal and vertical fluxes effects is a complicated issue, since the

two are connected. For example, the horizontal fluxes may impact the vertical effects by transporting sea ice, heat and moisture into the Polar Regions. On the other hand, the vertical fluxes effects, may impact the boundary layer height which in turn may have an impact on wind speed and direction that drives the horizontal effects.

3. Results and discussions

3.1. Quantifying the senssitivity between wind and sea ice concentration

We analyze SIC and 10 m wind speed using a monthly linear regression over 1979–2018. Note that areas with constant SIC are excluded. We found, in general, a significant relationship (p value < 0.05 from T-test) between increasing ERA5 (Hersbach *et al* 2020) wind speed and sea ice retreat, which in some locations and particular months may approach 100% (figure 1). Similar patterns, although with slightly different magnitude, are also found using wind data from the other five reanalyses both for the Arctic and the Antarctic regions (not shown). We note here that the ASR reanalysis product covers a shorter period (2000–2016) and therefore a different area of sea ice. In addition, reanalyses with a coarser resolution (e.g. NCEP_NCAR with 100-times larger grid cells than ERA5) may show lower correlation because of spatial compensatory effects on the temporal variation in SIC. Despite the slight differences between reanalysis products, the emerging correlation signal is consistent and statistically significant across the ensemble.

One may argue that such a correlation between wind speed and sea ice may originate from the long-term trends in both SIC and atmospheric circulation even without a clear relationship between the two parameters. To confute this hypothesis and prove the robustness of the relationship between the variables, we developed a new method to isolate the signal from short-term year-to-year variations (hereafter defined as inter-annual variations; see Methods). The key aspect of our methodology is that it assesses the variation between consecutive years of sea ice concentration to quantify the sensitivity to environmental drivers. This particular methodology that has been developed a few years ago (Alkama and Cescatti 2016), has several advantages:

- It factors out the long-term trend driven by climate change that generates a high collinearity of the variables under investigation.
- It factors out short-term variations (from days to weeks) that are related to the fast dynamics of the system and that have limited value in a climate change perspective.
- It takes advantage of the large climate variability on inter-annual time scales to quantify the sensitivities to environmental drivers.

Results obtained over the period 1979–2018 show that even at the year-to-year scale there is a consistent increase in wind speed (WS) with decreased SIC and vice-versa (figure 2). The largest increases are observed in autumn and winter: 46 ± 7% and 36 ± 5% over the Arctic and Antarctic regions, respectively. Given the large number of observations (i.e. pixels, figure S2) used in the analysis, the likelihood of isolating the effect of changes in sea ice from other potential drivers is high (figure S3). Consequently, the signal obtained is clear and symmetric for gaining and losing sea ice, indicating that the relationship between sea ice and WS is robust (figures 2 and S2, S3).

Analyzing the seasonal cycle of the sensitivity of the WS to SIC variability, we find that all the reanalysis products ERAinterim (Dee *et al* 2011), ERA5 (Hersbach *et al* 2020), NCEP_NCAR (Kalnay *et al* 1996), NCEP_DOE (Kanamitsu 2002), NCEP_CFSR (Saha *et al* 2010) and ASR (Bromwich *et al* 2018) and the median of the CMIP5 simulations exhibit a lower sensitivity of WS to SIC during late spring and summer for both the Arctic and Antarctic seas (figure 3). Different observed SIC datasets exist and locally may experience a big difference (Nose *et al* 2020). However, this difference is demonstrated to have little impact on our analysis (section 2.1 and figure S4). This may not, for example, explain the large difference between NCEP_CFSR and other reanalysis datasets. We would like to note here that it has been demonstrated that ERA5 produces the best reanalysis wind speed product over the Arctic (Graham *et al* 2019) and Antarctic (Dong *et al* 2020) regions, which is the reason why we decided to pay more attention to this product in the rest of the study. The same method has also been applied to 26 CMIP5 climate models. Overall, the median value from the 26 models captures quite well the seasonal pattern of the observed sensitivity but the spread among climate models is large and the magnitude is considerably lower, except for the model CanESM2 that shows a similar and in some months a slightly larger sensitivity (see the animation in the supplement). Specifically, the model MRI-CGCM3 shows a strong opposite sensitivity while the GFDL-CM3, GISS-E2-H-CC, GISS-E2-H, GISS-E2-R-CC and GISS-E2-R models show a very low or non-significant WS sensitivity to SIC in summer.

The seasonal cycle of sensitivity of the ERA5 wind gust (maximum hourly wind) to SIC is similar to the mean WS sensitivity, with generally a higher magnitude in winter and a lower magnitude during summer months, in both the Arctic and Antarctic seas (figure 3). With sea ice retreat, the maximum increase of 55 ± 5% in wind gust occurs during October to January over the Arctic Ocean, while the minimum increase of 23 ± 3% is observed in June. Over the Antarctic region, the maximum increase in gust of 42 ± 3% is observed in June and the minimum of

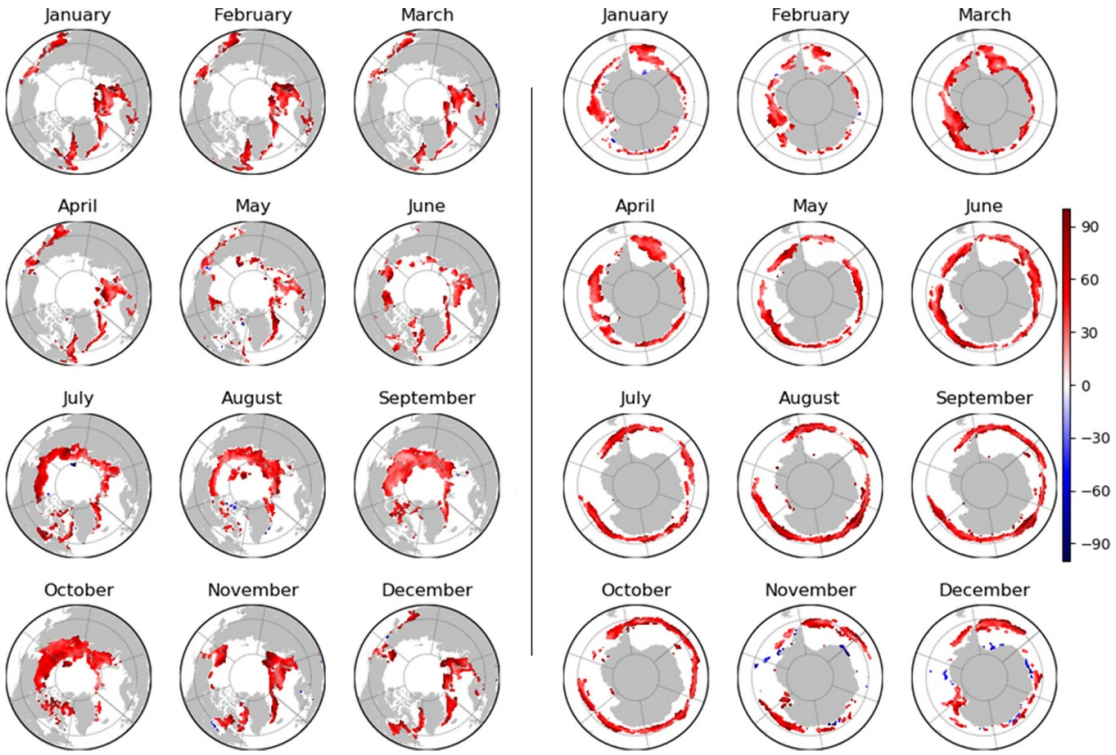

Figure 1. Percentage change in Arctic and Antarctic wind speed for a complete sea ice loss over areas with observed change in SIC during the 1979–2018 time period. Values are derived from the linear regression between normalized (0–100%, $WS_i = 100(WS_i - WS_{min})/(WS_{max} - WS_{min})$, where WS_{min} and WS_{max} represent the minimum and the maximum wind of the month being analyzed over 40 years) monthly mean ERA5 wind speed and observed sea ice concentration over 1979–2018. Only significant (based on T-test) slopes with p value < 0.05 are shown for $38 = 40-2$ degrees of freedom.

$8 \pm 2\%$ in December. This suggests that a reduction in atmospheric stability, which should be largest during autumn-winter, is a critical factor for driving stronger winds in areas of reduced sea ice (Mioduszewski *et al* 2018). Indeed, with sea ice loss, the boundary layer height and the 2 m air temperature increase in both Polar Regions, especially during autumn-winter (figures 4(e)–(h)). Another potential driver of WS is the change in surface pressure. Over the Arctic Ocean, years with less SIC correspond with years with lower surface pressure (figure 4(i)) especially in winter. This result is not observed, however, over the Antarctic region (figure 4(j)).

3.2. Causality between wind and sea ice concentration

To understand which component of the wind (i.e. meridional V or zonal U) is responsible for the observed WS increase with decreasing SIC, a similar analysis as in figure 3 was performed but for the two wind components (positive in the west-to-east and south-to-north directions). Results suggest that decreasing SIC over the Arctic is associated with a reduction in zonal wind speed over all seasons (figure 4(c)). Over the Antarctic, no clear pattern is observed during spring and winter while in summer and autumn a weaker zonal wind coincides with reduced sea ice cover (figure 4(d)). In the Antarctic sea, because of the absence of land around 60S, the dominant westerly winds (clockwise around the pole, figure S5) are stronger compared to the Northern hemisphere. And due to the presence of the Antarctic continent, sea ice is generally located in lower latitudes compared to Arctic sea ice. This may explain the opposite sign between the two hemispheres in August and October. Meridional wind shows a consistent pattern for both the Arctic and Antarctic seas, with increasing wind speed from lower to higher latitudes associated with the decline of SIC (figures 4(c) and (d)). The poleward wind sensitivity is generally larger than the zonal wind sensitivity, especially over the Antarctic region. Moreover, the seasonal shape of the meridional wind and wind speed sensitivities is similar. This result suggests that the correlation of sea ice reduction with increased surface wind speed is driven by the poleward (from lower to higher latitudes) wind component. This finding is of particular interest, since poleward winds are responsible for the advection of heat toward the poles. In fact, we show that the sea ice reduction is strongly linked to the increase of the atmospheric vertical integral of poleward heat flux (figures 4(k), (l) and S6) in both polar regions, which enhances the SIC sensitivity to wind. Altogether, these results clearly show that the surface wind speed increases with sea ice retreat and vice versa. However, this evidence cannot reveal which change comes first: stronger poleward wind or reduced ice cover.

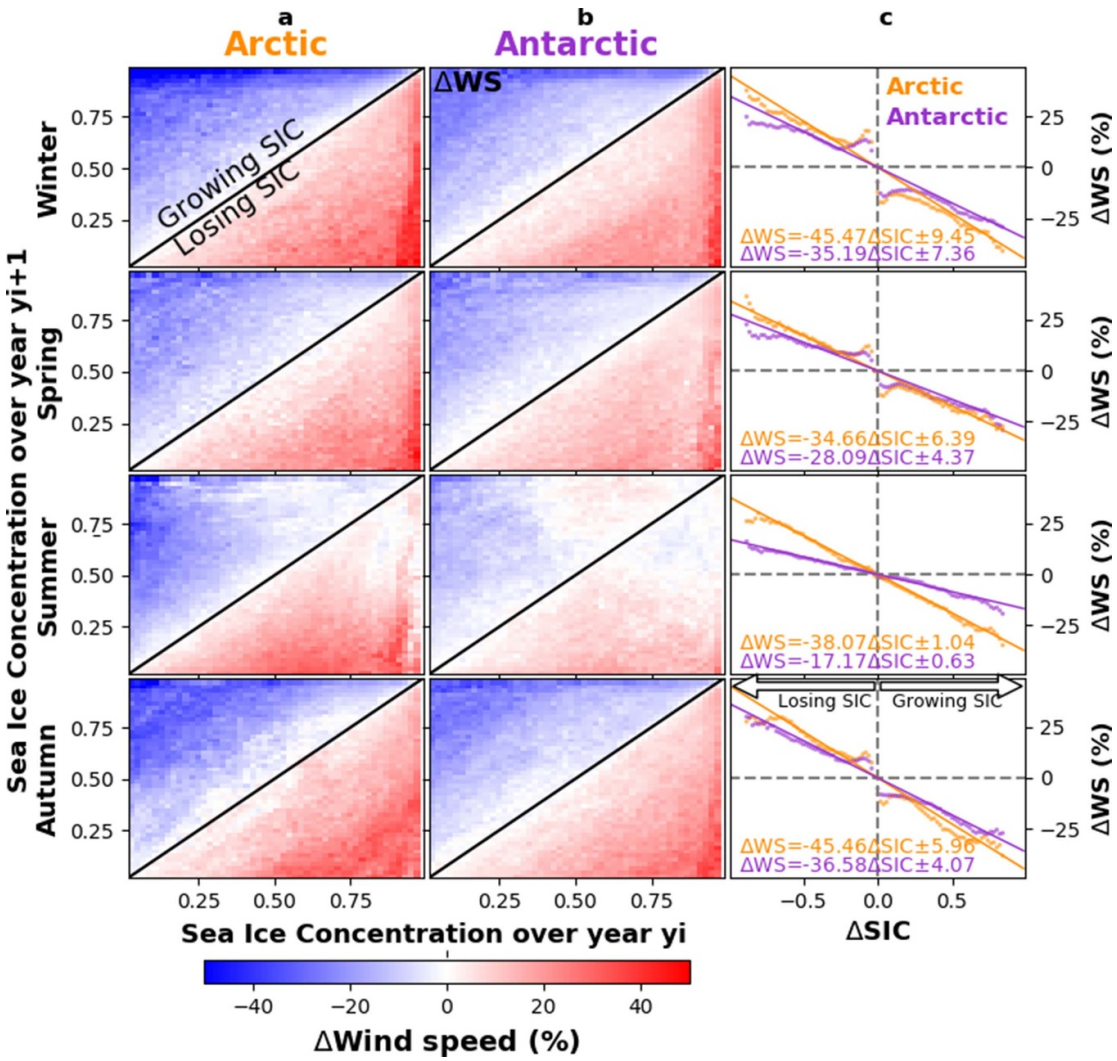

Figure 2. Seasonal changes of ERA5 wind speed (ΔWS) as a function of inter-annual variations in SIC. Percentage changes in seasonal wind speed (shown in blue and red colors) over the Arctic (left column) and Antarctic (middle column) as a function of SIC change between two consecutive years y_i (X-axis) and y_{i+1} (Y-axis) from 1979 to 2018. The graphs in these two columns are gridded in bins of 2% SIC in the range 0–1 on both axes. The plotted change of the 10 m wind speed data is calculated for each bin as average of all the grid points and year combinations, where ΔWS = WS(yi + 1) − WS(yi). The top triangles in these two columns represent cases of increasing SIC (i.e. SIC(yi + 1) > SIC(yi)), while the lower triangles represent cases of decreasing SIC (i.e. SIC(yi + 1) < SIC(yi)); the blue color indicates a reduction in 10 m WS, while red indicates an increase of WS. Each dot in the right column represents the average of one parallel to the diagonal in the left (shown by orange) or middle (shown by purple) columns, as described in the supplementary materials.

In order to investigate the causality in the observed processes we address the following two questions and hypotheses:

1. Is the monthly variability in polar wind driven by variability in SIC? The hypothesis is that a strong reduction of the sea ice area and thickness in all seasons may lead to a substantial thermodynamic influence on the overlying atmosphere due to the sharp increase in surface temperature. This is likely to affect wind regimes over the polar oceans owing to changes in atmospheric stability, surface roughness, and/or baroclinicity (Mioduszewski *et al* 2018).
2. Or is the variability in SIC driven by monthly variability in wind speed? The hypothesis is that increasing poleward wind may enhance poleward atmospheric and oceanic heat transport and consequently reduce SIC (thermic effect of wind on SIC). On the other hand, depending on the direction of wind, it may contribute to the expansion or contraction of sea ice (Rigor *et al* 2002, Rampal *et al* 2009) (sea ice movement/deformation resulting from a dynamic effect of wind on SIC). We have to note here that once sea ice has been moved poleward by the poleward winds, the extra open ocean acts as a heat source. The poleward atmospheric heat transports the expanded warm open ocean into the inner sea ice area and thus would amplify the thermal effect. Therefore, both dynamic and thermodynamic processes would be closely linked. In addition, wind may modify the atmospheric total water column and

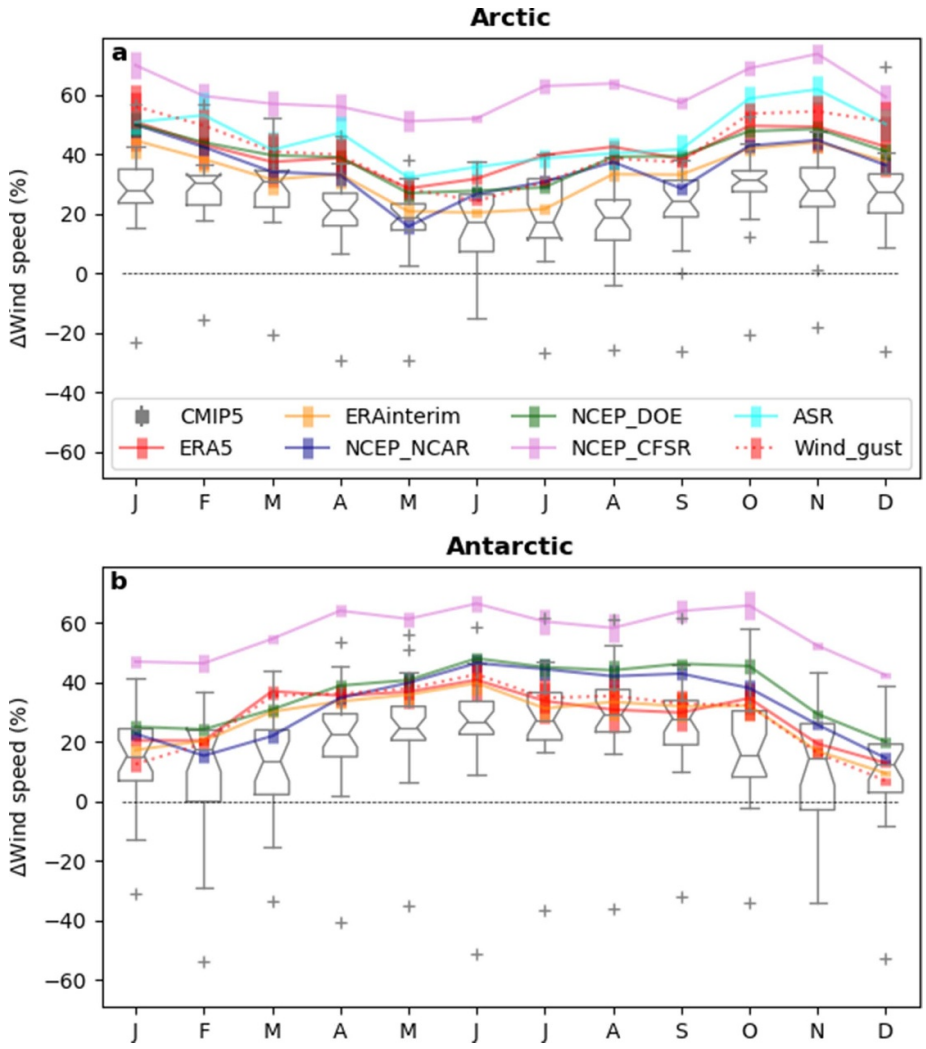

Figure 3. Monthly changes in 10 m mean wind speed and wind gust for a hypothetical 100% decrease in SIC over the areas where we observed SIC changes during the period 1979–2018. This estimate was derived by linear interpolation of the change of wind speed as a function of change in SIC using all possible combinations of pairs of consecutive years for a given month from 1979 to 2018 (except for ASR, that covers 2000–2016, and NCEP_CFSR, that covers 1979–2010) and for all grid cells for which SIC is larger than zero in one of the two years. Reanalyses are shown by solid lines (ERA5 red, ERAinterim orange, NCEP_NCAR blue, NCEP_DOE green, NCEP_CFSR purple and ASR cyan), where the standard deviation of the slopes is indicated by the colored rectangles. CMIP5 models are represented by grey boxplots, in which the box represents the first, second (median) and third quartiles (whiskers indicate the 99% confidence interval and grey markers (plus) show outliers).

surface albedo, and both of them may clearly impact SIC mainly via the NSR (Taylor *et al* 2013, Gong *et al* 2017) and via surface turbulent fluxes (Park *et al* 2015b, Woods and Caballero 2016).

To address these two questions we applied a Granger causality test (Granger 1969) between the two monthly time series (WS and SIC), in which the mean seasonal cycle is removed. We find that wind significantly (p value < 0.05) leads to SIC changes across the entire spatial domain of the analysis with an optimal lag of +2 months (figures 5(a) and (b)) which is in agreement with a previous study (Ogi *et al* 2010) that demonstrated that wind-forcing in the Arctic explains 50% of the inter-annual September Arctic sea ice variability and about 1/3 of the downward linear trend of sea ice over the past 31 years. This is also in agreement with another study (Kapsch *et al* 2019), which suggested that transport of heat and moisture into the Arctic during spring enhances the annual melt onset, setting the stage for the September ice minimum. Such diminishing sea ice with its associated albedo feedback has had a leading role in recent Arctic temperature amplification (Screen and Simmonds 2010). This suggests that the second hypothesis is likely to be correct. On the other hand we also find that changes in SIC lead to changes in wind over about half of the spatial domain (figures 5(c) and (d)), with an optimal lag of one month in general. This suggests that the first hypothesis may also hold locally, with SIC changes causing variations in near-surface wind speed. This may be due to the near-surface warming induced by sea ice reduction that would increase the boundary layer height (reduce atmospheric stability) and in turn increase the wind

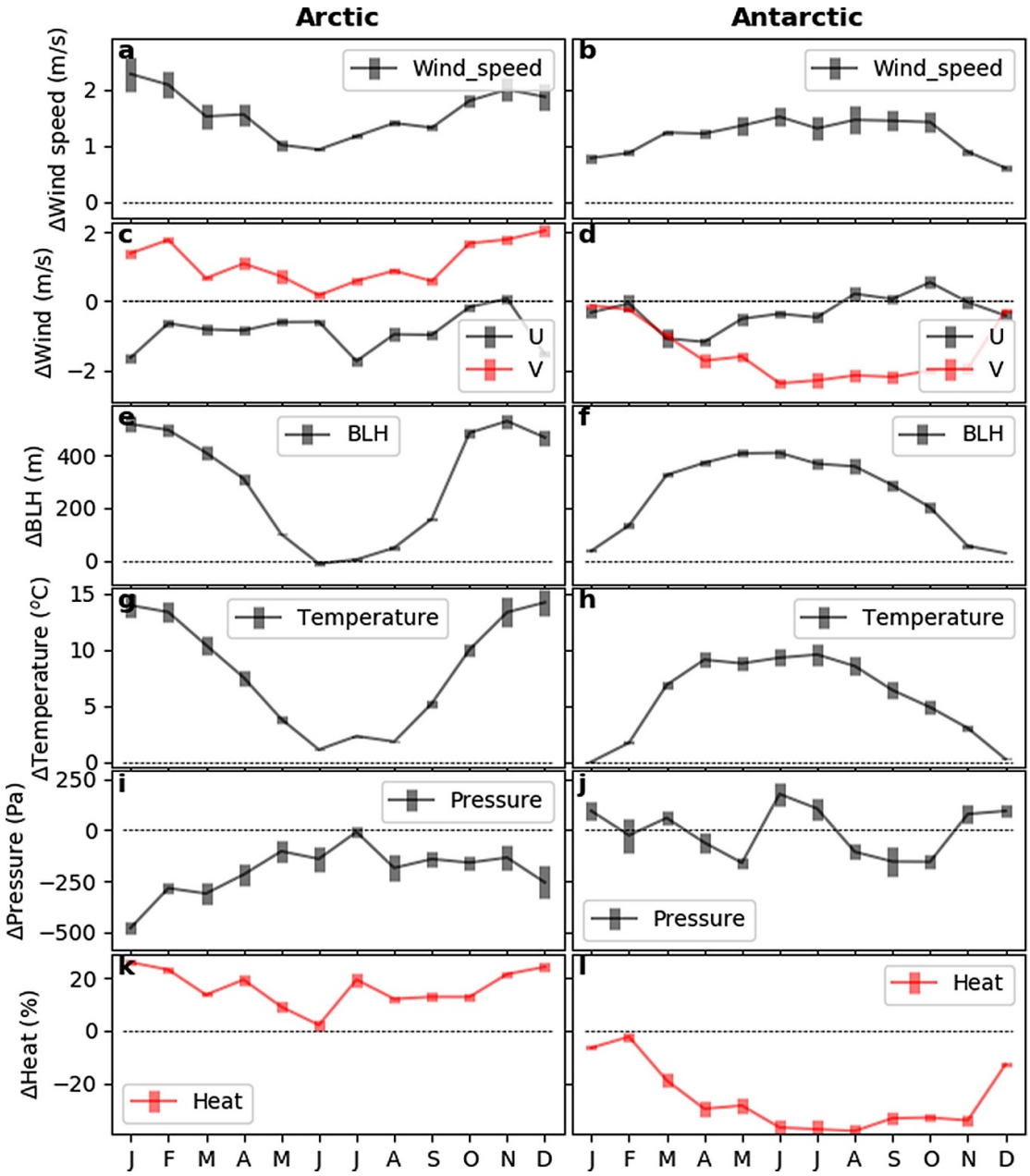

Figure 4. Monthly changes in 10 m wind speed, zonal wind ('U' positive in the West–East direction), meridional wind ('V' positive in the south–north direction), boundary layer height (BLH), 2 m air temperature, surface pressure and vertical integral of atmospheric northward heat flux (positive in the south–north direction) for a hypothetical 100% decrease in SIC over the areas where we observed SIC change during the period 1979–2018. These estimates were derived from linear interpolation of the change of ERA5 wind speed and other variables as a function of change in SIC resulting from all possible combinations of pairs of consecutive years for any given month from 1979 to 2018 and for all grid cells for which SIC is larger than zero in one of the two years. The thick bars represent the standard error of the slope.

speed. Altogether, the results of the causality analysis show that polar sea ice and wind positively interact in a two-way mode that may substantially amplify the overall impact on sea ice loss through an enhancement of the warming and dynamic effects of poleward winds. This strong positive feedback in the interplay between winds and sea ice undoubtedly contributes to the polar amplification of climate warming.

3.3. Relative importance of wind impacts (dynamic, heat transport, radiative and turbulent fluxes) on sea ice concentration

To estimate which of the large-scale horizontal fluxes (OHF, AHF, Dynamic) and local vertical fluxes (NSR, Turbulent) predictors is dominating the SIC change, we used the relative importance index (see section 2.9). Our analysis shows clearly that OHF is dominating the horizontal effects of wind on SIC change (Fig. 6ab) in both Polar Regions and accounts for 66% (79%) in the Arctic (Antarctic), followed by AHF that accounts for 28% (18%) while the Dynamic effect plays a marginal role with only 6% (3%) of the total horizontal effects. But as discussed before, these horizontal effects induce two vertical effects that show a clear seasonal cycle (figures 6(c) and (d)). NSR dominates the spring and summer while turbulent fluxes are dominant during autumn and winter.

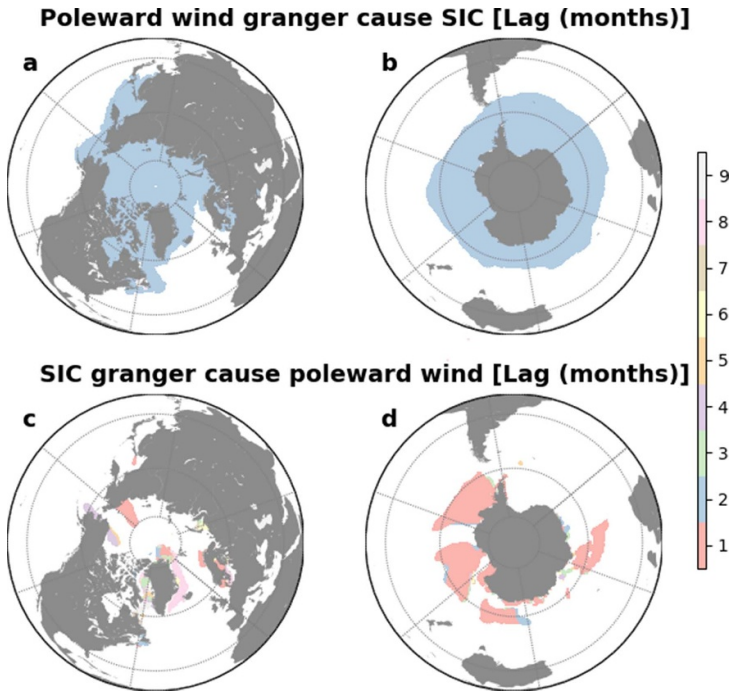

Figure 5. Optimal lag (in months) from Granger causality test. Only lags with significant *F*-test (p value < 0.05) are shown.

When combining all effects together, our analysis shows clearly that local vertical effects are dominant. Indeed, the radiative predictor dominates (NSR ∼95%) the summer SIC change in both polar regions (figures 6(e), (f)). This is consistent with previous studies (Screen and Simmonds 2010, Kashiwase *et al* 2017) that pointed out the importance of sea ice albedo for warming the surface of the Arctic ocean, especially during the summer period. However, in winter, where solar radiation is absent or very low, change in clouds and atmospheric moisture dominate the observed change in NSR since the role of albedo becomes insignificant. Indeed, our analysis shows that with sea ice retreat, due to an increase of the poleward wind, the poleward latent heat transport increases by up to 50% in the Arctic and by up to 45% in the Antarctic seas (figure S7), which may reduce SIC especially during winter by absorbing and emitting back to the surface part of the upward surface thermal radiation (Taylor *et al* 2013, Gong *et al* 2017). However this effect is marginal compared to the role played by turbulent heat fluxes in autumn and winter that may be caused by poleward heat and moisture transport. This is consistent with previous studies that demonstrated the role of moisture transport and sensible heat flux on the Arctic sea ice retreat (Park *et al* 2015a, Vihma *et al* 2016, Woods and Caballero 2016). During autumn and winter (from September to March) over Arctic regions, heat transport plays a small role (but higher than in other months) that accounts for 3% to 7% of the change in SIC and is almost equally distributed between the atmosphere and the ocean. However, over austral autumn and winter (mainly from April to August), heat transport in the Antarctic plays a non-negligible role (between 20% and 30%). At the seasonal cycle scale, it was demonstrated (Holland and Kwok 2012) that wind-driven changes in ice advection are the dominant driver of SIC trends around much of West Antarctica, whereas wind-driven thermodynamic changes dominate elsewhere. However, our analysis shows a very limited effect of the dynamic role of wind in both Polar Regions, with generally less than 1% except during autumn and winter, for which the values range from 1% to a maximum of 2%. But as mentioned before, both the dynamic, thermodynamic, turbulent and radiative processes are closely linked. For example, both the dynamic and thermodynamic processes have an impact on SIC which in turn impacts the radiative and turbulent processes, which clearly creates a positive feedback between the four processes.

4. Conclusion

Our results clearly show strong relationships between near-surface wind speed and sea ice concentration that are consistent among the reanalysis datasets, such that less ice cover is associated with stronger winds. In addition, this study unveils some of the mechanisms that link wind and sea ice cover, demonstrating that the poleward wind component is particularly relevant, because it enhances the poleward moisture and heat flux and boosts the polar sea ice loss even in some cases where a change in SIC precedes the change in wind speed. Climate models on

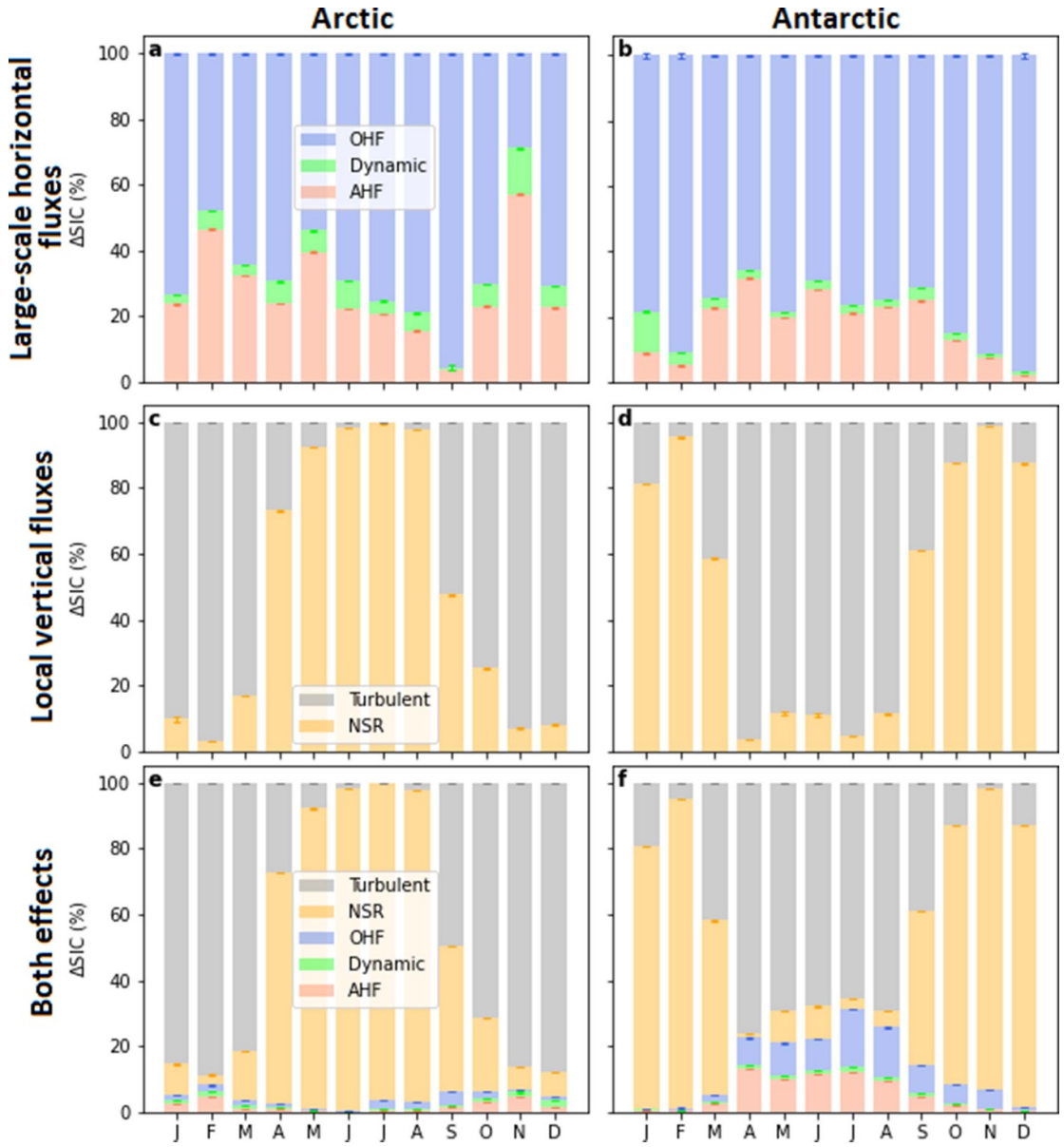

Figure 6. Relative importance of large-scale horizontal fluxes (a), (b), local vertical fluxes (c), (d) and both (e), (f) effects of wind on SIC. Relative importance of ocean heat flux (OHF), convergence/divergence of sea ice (dynamic), atmospheric heat flux (AHF), net surface radiation (NSR), surface turbulent fluxes and their associated standard error on the change of sea ice concentration (SIC).

average produce similar patterns, but with a large spread in magnitude and even sign of the relationship. In addition to the thermal and dynamical effects of wind, enhanced poleward heat and moisture transport may also drive sea ice retreat via turbulent flux (Park *et al* 2015a, Woods and Caballero 2016, Vihma *et al* 2016). Our analysis shows that such local vertical effects may explain 87% of the winter (December–January–February) Arctic SIC change and 67% of winter (June–July–August) Antarctic SIC change. The poleward ocean and atmosphere heat transport plays also an important role for the winter Arctic (5%) and Antarctic (25%) SIC change. During summers, a small change in SIC (albedo) that can be caused by the dynamic or thermal transport effect is strongly exacerbated by the large solar input. This is the reason why the local NSR is shown to be responsible for a large part of SIC change.

Future projections of sea ice concentration are uncertain not only because of unknown emission trajectories of greenhouse gases, but also due to the multiple and relevant pathways through which sea ice feeds back onto the Earth's climate system (Arzel *et al* 2006, Zhang and Walsh 2006). Discovering the reasons behind the large spread of simulated warming and sea ice loss among climate models is a scientific challenge that has large consequences for future climate strategies and policies (Turner *et al* 2013, Simmonds 2015, Holland *et al* 2017). As an example of uncertainty, in this study the MRI-CGM3 model, which shows an opposite sensitivity of wind to SIC compared to that derived from remote sensing

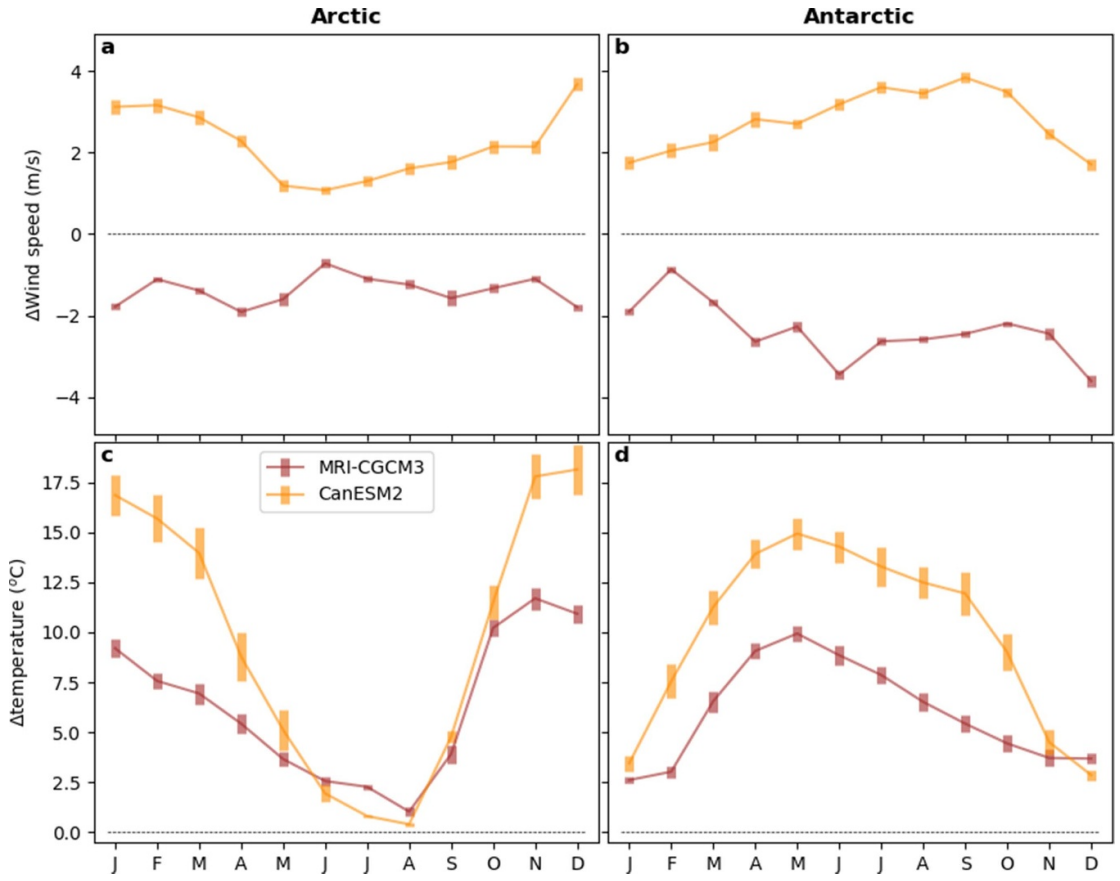

Figure 7. Monthly change in 10 m wind and 2 m air temperature for a hypothetical 100% decrease in SIC over the areas where we observed SIC change during the period 1979–2018. This change estimate was derived from the use of a linear interpolation of the change of wind speed and 2 m air temperature as a function of change in SIC resulting from all possible combinations of pairs of consecutive years for a given month from 1979 to 2018 and for all grid cells for which SIC is larger than zero in one of the two years. All the analysis are based on the two extreme CMIP5 models MRI-CGCM3 (the only model showing negative sensitivity of wind to SIC) and CanESM2 (the model showing the highest positive sensitivity of wind to SIC that is similar to reanalysis).

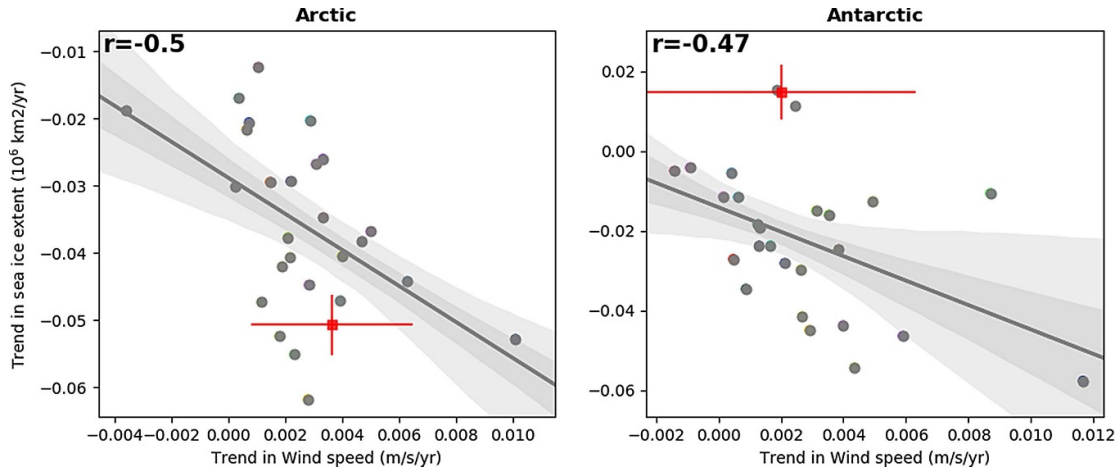

Figure 8. Linear regression (grey solid line and its 68% (dark grey envelope) and 95% (light grey envelope) confidence interval) between: the trend in wind speed and trend in sea ice concentration of the 26 CMIP5 climate models shown by grey dots over 1979–2018. The observed and reanalysis trends are shown by red colors where the confidence interval refers to the standard error of the trend.

and reanalyses (figures 7(a) and (b)), produces a 5 °C weaker warming for a complete sea ice retreat over the areas with observed SIC change during the last 40 years than the model CanESM3, which shows the most realistic sensitivity of wind and 2 m air temperature to SIC (figures 7(c) and (d), and for a comparison with the ERA5 reanalysis figures 4(g) and (h)).

In conclusion, we believe that the robustness of our results, which are stemming from evidence-driven analysis, is substantially reducing the uncertainty regarding the covariation between polar wind and sea ice, and improving our understanding of present and future polar climates. For example, our results show that models that simulate a larger trend in SIC are also those simulating larger trends in wind speed (figure 8). Ultimately, these findings regarding the interplay between wind and sea ice variability may lead to an improved model representation of the wind-sea ice feedback, a mechanism that is likely to affect the speed of the polar sea ice retreat, which in turn has a broad impact on the global climate system (Deser *et al* 2015, England *et al* 2020).

Acknowledgments

The authors acknowledge the use of NCEP_NCAR and NCEP_DOE Reanalysis Derived data provided by the NOAA/OAR/ESRL PSD, Boulder, Colorado, USA; the ASR reanalysis project carried out by the National Center for Atmospheric Research and Byrd Polar and Climate Research Center of The Ohio State University; the ERAinterim and ERA5 Reanalysis project carried out by the European Centre for Medium-Range Weather Forecasts (ECMWF) generated using Copernicus Climate Change Service Information 2019, as well as the modeling groups that contributed to the CMIP5 data archive. This work was supported by European Commission Joint Research Centre. TV was supported by the Academy of Finland (contract 304345).

Author contributions

R.A directed this work with contributions from all authors. R A and E N K performed the analysis. All authors discussed the results and contributed to writing the paper.

Conflict of interest

The authors declare no competing financial interests.

Data availability statement

The data that support the findings of this study are openly available. OSI-SAF sea ice concentration is accessible at (https://cds.climate.copernicus.eu/cdsapp#!/dataset/satellite-seaice?tab=overview). Bootstrap sea ice concentration is accessible at http://nsidc.org/data/G02202. ERAinterim is accessible at http://www.ecmwf.int/en/forecasts/datasets/reanalysis-datasets/era-interim. ERA5 is accessible at http://climate.copernicus.eu/climate-reanalysis. NCEP_NCAR is accessible at http://www.esrl.noaa.gov/psd/data/gridded/data.ncep.reanalysis.derived.surface.html. NCEP_DOE is accessible at https://rda.ucar.edu/datasets/ds091.0/. NCEP_CFSR is accessible at https://climatedataguide.ucar.edu/climate-data/climate-forecast-system-reanalysis-cfsr. ASR is accessible at https://climatedataguide.ucar.edu/climate-data/arctic-system-reanalysis-asr. CMIP5 is accessible at https://esgf-node.llnl.gov/search/cmip5/.

Additional information

The programs used to generate all the results are made with Python. Analysis scripts are available by request to R. Alkama.

ORCID iDs

Ernest N Koffi https://orcid.org/0000-0002-7692-4328
Timo Vihma https://orcid.org/0000-0002-6557-7084

References

Alkama R and Cescatti A 2016 Climate change: biophysical climate impacts of recent changes in global forest cover *Science* **351** 600–4
Alkama R, Taylor P C, Garcia-San Martin L, Douville H, Duveiller G, Forzieri G, Swingedouw D and Cescatti A 2020 Clouds damp the radiative impacts of polar sea ice loss *Cryosphere* **14** 2673–86
Arzel O, Fichefet T and Goosse H 2006 Sea ice evolution over the 20th and 21st centuries as simulated by current AOGCMs *Ocean Modelling* **12** 401–15
Blunden J, Arndt D S, Blunden J and Arndt D S 2012 State of the climate in 2011 *Bull. Am. Meteorol. Soc.* **93** S1–282
Boisvert L N, Markus T and Vihma T 2013 Moisture flux changes and trends for the entire Arctic in 2003-2011 derived from EOS Aqua data *J. Geophys. Res. Ocean* **118** 5829–43
Bromwich D H *et al* 2018 The Arctic system reanalysis, version 2 *Bull. Am. Meteorol. Soc.* **99** 805–28
Caesar L, Rahmstorf S, Robinson A, Feulner G and Saba V 2018 Observed fingerprint of a weakening Atlantic Ocean overturning circulation *Nature* **556** 191–6
Cao Y, Liang S, Chen X, He T, Wang D and Cheng X 2017 Enhanced wintertime greenhouse effect reinforcing Arctic amplification and initial sea-ice melting *Sci. Rep.* **7** 8462
Chylek P, Folland C K, Lesins G, Dubey M K and Wang M 2009 Arctic air temperature change amplification and the Atlantic multidecadal oscillation *Geophys. Res. Lett.* **36** L14801
Cohen J *et al* 2014 Recent Arctic amplification and extreme mid-latitude weather *Nat. Geosci.* **7** 627–37
Comiso J C, Comiso J C, Parkinson C L, Gersten R, Stock L, Parkinson C L, Gersten R and Stock L 2008 Accelerated decline in the arctic sea ice cover *Geophys. Res. Lett.* **35** 01703
Dee D P *et al* 2011 The ERA-Interim reanalysis: configuration and performance of the data assimilation system *Q. J. R. Meteorol. Soc.* **137** 553–97
Deser C, Tomas R A and Sun L 2015 The role of ocean-atmosphere coupling in the zonal-mean atmospheric response to Arctic sea ice loss *J. Clim.* **28** 2168–86
Ding Q *et al* 2019 Fingerprints of internal drivers of Arctic sea ice loss in observations and model simulations *Nat. Geosci.* **12** 28–33

Dong X, Wang Y, Hou S, Ding M, Yin B and Zhang Y 2020 Robustness of the recent global atmospheric reanalyses for Antarctic near-surface wind speed climatology *J. Clim.* **33** 4027–43

Dore M H I 2005 Climate change and changes in global precipitation patterns: what do we know? *Environ. Int.* **31** 1167–81

England M R, Polvani L M, Sun L and Deser C 2020 Tropical climate responses to projected Arctic and Antarctic sea-ice loss *Nat. Geosci.* **13** 275–81

England M, Jahn A and Polvani L 2019 Nonuniform contribution of internal variability to recent Arctic sea ice loss *J. Clim.* **32** 4039–53

Francis J A, Hunter E, Zou C-Z, Francis J A, Hunter E and Zou C-Z 2005 Arctic tropospheric winds derived from TOVS satellite retrievals *J. Clim.* **18** 2270–85

Gong T, Feldstein S and Lee S 2017 The role of downward infrared radiation in the recent arctic winter warming trend *J. Clim.* **30** 4937–49

Graham R M, Hudson S R and Maturilli M 2019 Improved performance of ERA5 in Arctic gateway relative to four global atmospheric reanalyses *Geophys. Res. Lett.* **46** 2019GL082781

Granger C W J 1969 Investigating causal relations by econometric models and cross-spectral methods *Econometrica* **37** 424

Graversen R G, Mauritsen T, Tjernström M, Källén E and Svensson G 2008 Vertical structure of recent Arctic warming *Nature* **451** 53–56

Grömping U 2006 Relative importance for linear regression in R: the package relaimpo *J. Stat. Softw.* **17** 1–27

Hansen J, Sato M and Ruedy R 1997 Radiative forcing and climate response *J. Geophys. Res. Atmos.* **102** 6831–64

Hersbach H *et al* 2020 The ERA5 global reanalysis *Q. J. R. Meteorol. Soc.* **146** 1999–2049

Holland M M, Landrum L, Raphael M and Stammerjohn S 2017 Springtime winds drive Ross Sea ice variability and change in the following autumn *Nat. Commun.* **8** 731

Holland P R and Kwok R 2012 Wind-driven trends in Antarctic sea-ice drift *Nat. Geosci.* **5** 872–5

Jakobson L, Vihma T and Jakobson E 2019 Relationships between sea ice concentration and wind speed over the Arctic Ocean during 1979–2015 *J. Clim.* **32** 7783–96

Kalnay E *et al* 1996 The NCEP/NCAR 40-year reanalysis project *Bull. Am. Meteorol. Soc.* **77** 437–71

Kanamitsu M *et al* 2002 NCEP-DEO AMIP-II reanalysis (R-2) *Bull. Am. Meteorol. Soc.* **83** 1631–44

Kapsch M-L, Skific N, Graversen R G, Tjernström M and Francis J A 2019 Summers with low Arctic sea ice linked to persistence of spring atmospheric circulation patterns *Clim. Dyn.* **52** 2497–512

Kashiwase H, Ohshima K I, Nihashi S and Eicken H 2017 Evidence for ice-ocean albedo feedback in the Arctic Ocean shifting to a seasonal ice zone *Sci. Rep.* **7** 1–10

Kay J E, Holland M M and Jahn A 2011 Inter-annual to multi-decadal Arctic sea ice extent trends in a warming world *Geophys. Res. Lett.* **38** 15708

Kirtman B *et al* 2013 Near-term climate change: projections and predictability *Climate Change 2013: The Physical Science Basis. Contribution of Working Group I to the Fifth Assessment Report of the Intergovernmental Panel on Climate Change*, ed T F Stocker, D Qin, G-K Plattner, M Tignor, S K Allen, J Boschung, A Nauels, Y Xia, V Bex and P M Midgley (Cambridge: Cambridge University Press) (www.ipcc.ch/site/assets/uploads/2018/02/WG1AR5_Chapter11_FINAL.pdf)

Lindsay R, Wensnahan M, Schweiger A and Zhang J 2014 Evaluation of seven different atmospheric reanalysis products in the Arctic* *J. Clim.* **27** 2588–606

Maksym T 2019 Arctic and Antarctic Sea ice change: contrasts, commonalities, and causes *Annu. Rev. Mar. Sci.* **11** 187–213

Mioduszewski J, Vavrus S, Wang M, Mioduszewski J, Vavrus S and Wang M 2018 Diminishing Arctic Sea ice promotes stronger surface winds *J. Clim.* **31** 8101–19

Nakanowatari T, Inoue J, Sato K and Kikuchi T 2015 Summertime atmosphere-ocean preconditionings for the Bering Sea ice retreat and the following severe winters in North America *Environ. Res. Lett.* **10** 094023

Nakanowatari T, Sato K and Inoue J 2014 Predictability of the Barents Sea ice in early winter: remote effects of oceanic and atmospheric thermal conditions from the North Atlantic *J. Clim.* **27** 8884–901

Nicholls R J and Cazenave A 2010 Sea-level rise and its impact on coastal zones *Science* **328** 1517–20

Nose T, Waseda T, Kodaira T and Inoue J 2020 Satellite-retrieved sea ice concentration uncertainty and its effect on modelling wave evolution in marginal ice zones *Cryosphere* **14** 2029–52

Ogi M, Yamazaki K and Wallace J M 2010 Influence of winter and summer surface wind anomalies on summer Arctic sea ice extent *Geophys. Res. Lett.* **37** 07701

Oort A H and Peixóto J P 1983 Global angular momentum and energy balance requirements from observations *Adv. Geophys.* **25** 355–490

Overland J E and Wang M 2010 Large-scale atmospheric circulation changes are associated with the recent loss of Arctic sea ice *Tellus A Dyn. Meteorol. Oceanogr.* **62** 1–9

Park H S, Lee S, Son S W, Feldstein S B and Kosaka Y 2015a The impact of poleward moisture and sensible heat flux on arctic winter sea ice variability *J. Clim.* **28** 5030–40

Park H-S, Lee S, Kosaka Y, Son S-W, Kim S-W, Park H-S, Lee S, Kosaka Y, Son S-W and Kim S-W 2015b The impact of Arctic winter infrared radiation on early summer sea ice *J. Clim.* **28** 6281–96

Parkinson C L 2019 A 40-y record reveals gradual Antarctic sea ice increases followed by decreases at rates far exceeding the rates seen in the Arctic *Proc. Natl Acad. Sci. USA* **116** 14414–23

Rampal P, Weiss J and Marsan D 2009 Positive trend in the mean speed and deformation rate of Arctic sea ice, 1979–2007 *J. Geophys. Res.* **114** C05013

Rigor I G, Wallace J M, Colony R L, Rigor I G, Wallace J M and Colony R L 2002 Response of sea ice to the Arctic oscillation *J. Clim.* **15** 2648–63

Saha S *et al* 2010 The NCEP climate forecast system reanalysis *Bull. Am. Meteorol. Soc.* **91** 1015–57

Sato K, Inoue J and Watanabe M 2014 Influence of the Gulf Stream on the Barents Sea ice retreat and Eurasian coldness during early winter *Environ. Res. Lett.* **9** 084009

Screen J A and Simmonds I 2010 The central role of diminishing sea ice in recent Arctic temperature amplification *Nature* **464** 1334–7

Simmonds I 2015 Comparing and contrasting the behaviour of Arctic and Antarctic sea ice over the 35 year period 1979-2013 *Ann. Glaciol.* **56** 18–28

Smetacek V and Nicol S 2005 Polar ocean ecosystems in a changing world *Nature* **437** 362–8

Srokosz M A and Bryden H L 2015 Observing the Atlantic Meridional Overturning Circulation yields a decade of inevitable surprises *Science* **348** 1255575–1255575

Stirling I 1997 The importance of polynyas, ice edges, and leads to marine mammals and birds *J. Mar. Syst.* **10** 9–21

Stott P 2016 How climate change affects extreme weather events *Science* **352** 1517–8

Taylor K E, Stouffer R J and Meehl G A 2012 An overview of CMIP5 and the experiment design *Bull. Am. Meteorol. Soc.* **93** 485–98

Taylor P C, Cai M, Hu A, Meehl J, Washington W and Zhang G J 2013 A decomposition of feedback contributions to polar warming amplification *J. Clim.* **26** 7023–43

Thornalley D J R *et al* 2018 Anomalously weak Labrador Sea convection and Atlantic overturning during the past 150 years *Nature* **556** 227–30

Turner J, Bracegirdle T J, Phillips T, Marshall G J, Hosking J S, Turner J, Bracegirdle T J, Phillips T, Marshall G J and

Hosking J S 2013 An initial assessment of Antarctic Sea ice extent in the CMIP5 models *J. Clim.* **26** 1473–84

Vihma T 2014 Effects of Arctic Sea ice decline on weather and climate: a review *Surv. Geophys.* **35** 1175–214

Vihma T, Screen J, Tjernström M, Newton B, Zhang X, Popova V, Deser C, Holland M and Prowse T 2016 The atmospheric role in the Arctic water cycle: a review on processes, past and future changes, and their impacts *J. Geophys. Res. Biogeosci.* **121** 586–620

Woods C and Caballero R 2016 The role of moist intrusions in Winter Arctic warming and sea ice decline *J. Clim.* **29** 4473–85

Zhang X, Sorteberg A, Zhang J, Gerdes R and Comiso J C 2008 Recent radical shifts of atmospheric circulations and rapid changes in Arctic climate system *Geophys. Res. Lett.* **35** L22701

Zhang X and Walsh J E 2006 Toward a seasonally ice-covered Arctic Ocean: scenarios from the IPCC AR4 model simulations *J. Clim.* **19** 1730–47